Isolated cavities dominate Greenland Ice Sheet dynamic response to lake drainage.

J. Z. Mejia[1], J. D. Gulley[1], C. Trunz[2], M. D. Covington[2], T. C. Bartholomaus[3], S. Xie[4], T. Dixon[1]

[1]Department of Geosciences, University of South Florida, 4202 E. Fowler Ave. Tampa, FL 33620.
[2]Department of Geosciences, University of Arkansas, 1 University of Arkansas, Fayetteville, AR 72701
[3]Department of Geological Sciences, University of Idaho, 875 Perimeter Drive, Moscow, ID 83844
[4]Scripps Institution of Oceanography, University of California San Diego, 9500 Gilman Drive, MC 0225, La Jolla, CA 92093

Key Points:

- Isolated cavity drainage governs Greenland Ice Sheet slowdowns, not increased drainage system efficiency.
- Floodwaters from rapid supraglacial lake drainages induce widespread slowdowns by dewatering isolated cavities.
- Ice sliding speeds may be more sensitive to persistent meltwater inputs than previously thought.

Corresponding author: Jessica Mejia, jessicamejia@usf.edu

Abstract

Seasonal variability in the Greenland Ice Sheet's (GrIS) sliding speed is regulated by the response of the subglacial drainage system to meltwater inputs. However, the importance of channelization relative to the dewatering of isolated cavities in controlling seasonal ice deceleration remains unsolved. Using ice velocity, moulin hydraulic head, and glacio-hydraulic tremor measurements we show the passing of a subglacial floodwave following the drainage of an up-glacier supraglacial lake slowed minimum sliding speeds to wintertime background values without increasing the hydraulic capacity of the moulin-connected drainage system. We interpret these results to reflect a persistent basal traction increase consistent with the dewatering of isolated cavities exert the dominant control on seasonal ice velocity decreases. Current predictions of the GrIS's ice-dynamic response to increased surface melting hinges on the subglacial drainage system's ability to increase its capacity to offset sustained meltwater influxes, which our results demonstrate may not be the case.

Plain Language Summary

Meltwater produced on the surface of the Greenland Ice Sheet reaches the bed by flowing into crevasses or moulins, vertical conduits that reach the base of the ice sheet. Early in the summer, meltwater that reaches the bed increases water pressures within the drainage system underneath the ice sheet and increasing sliding speeds. However, later in the summer, ice sliding speeds often slowdown despite continued meltwater inputs. While these slowdowns have been attributed to the growth of channels that connect to moulins, recent observations suggest the drainage of hydraulically isolated cavities, pockets of water that form on the lee-side of bedrock bumps, may instead be responsible. Here we use measurements ice velocity and water pressures within moulins several kilometers away from rapidly draining supraglacial lakes to show that the passing of the floodwave underneath the ice-sheet slowed sliding to winter-time speeds without enlarging subglacial channels. Instead, our results indicate that the drainage of isolated cavities is responsible for slowdowns that occur during the melt season. Because the growth of subglacial channels was thought to be able to compensate for increased melting, our results suggest the Greenland Ice Sheet's ice-dynamic contribution to sea level rise may be significantly underestimated.

1 Introduction

Predicting the Greenland Ice Sheet's (GrIS) response to future climate warming scenarios is limited by gaps in understanding links between ice sheet hydrology and dynamics. Using better-studied alpine glaciers as GrIS analogs, the subglacial drainage system's hydraulic capacity is considered the primary control on sliding speeds. Ice accelerates when water inputs exceed the drainage system's hydraulic capacity, causing water to back-up englacially, which increases the pressure head at the bed and reduces basal traction (Bartholomew et al., 2012; Bartholomaus et al., 2007). Ice velocity decreases during the melt season have been interpreted to reflect a transition from an inefficient, distributed drainage system consisting of high-pressure linked cavities and till aquifers to an efficient drainage system consisting of low-pressure conduits (Sundal et al., 2011; Sole et al., 2013; Chandler et al., 2013; Colgan et al., 2011). Conduits are thought to be able to enlarge in order to accommodate sustained meltwater influxes and drain water from the surrounding inefficient drainage system, thereby reducing subglacial water pressures and slowing sliding speeds. Under this paradigm, the GrIS ice-dynamic response to future warming should be buffered by conduit enlargement.

Recent observations have shown that weakly connected, and hydrologically isolated cavities can drive seasonal decreases in ice velocity that have been widely attributed to increased drainage system efficiency. The isolated drainage system consists of water-filled

cavities which form on the lee side of bedrock bumps where sliding decouples ice from the bed (Lliboutry, 1968; Walder, 1986; Iken & Truffer, 1997). Isolated cavities exist between, and are isolated from, distributed and channelized regions of the subglacial drainage system, similar to how oxbow or thermokarst lakes and ponds are disconnected from nearby rivers and streams in surficial hydrological systems. Distributed and channelized parts of the drainage system modulate pressures within isolated cavities indirectly through the transfer of mechanical support (Murray & Clarke, 1995; Meierbachtol et al., 2016), or through sliding-driven fluctuations cavity volume(Iken & Truffer, 1997). Because pressures within isolated cavities are high, these small changes in cavity volume cause water pressures to fluctuate about ice overburden pressure, modifying basal traction and modulating sliding where they are distributed over large areas of the bed (Andrews et al., 2014; Hoffman et al., 2016; Iken & Truffer, 1997; Meierbachtol et al., 2016).

Isolated cavities can connect and drain into the distributed drainage system when large influxes of water overwhelm the subglacial drainage system. Rapid basal sliding or hydraulic jacking of the ice can create transient connections between isolated cavities and nearby parts of the distributed drainage system. If isolated cavities are at higher pressure, water in them will drain into the distributed system until connections subsequently close-off when water pressures are low (Iken & Truffer, 1997; Stone & Clarke, 1996; Rada & Schoof, 2018). Consequently, isolated cavities that maintained high average subglacial water pressure and promoted sliding before the connection would have lower water pressures and therefore slowing sliding speeds. If drainage of isolated cavities is responsible for observed slowdowns (Andrews et al., 2014; Hoffman et al., 2016; Ryser et al., 2014; Hoffman et al., 2011), and not increased channelization, it is less clear how the GrIS will respond to future warming.

2 Study Site and Data

2.1 Study Area

Here we report how relationships between subglacial water pressure and ice sliding speeds changed when rapidly draining supraglacial lakes triggered a subglacial flood-wave that passed beneath our study site on the GrIS. Using those changes, we infer that the dewatering of isolated cavities, not increased channelization, is responsible for seasonal decreases in ice velocity. We established a camp in the ablation area of Sermeq Avannarleq on the western GrIS (Fig. 1; 65.6°N, 49.7°W), more than 7 km downglacier from several supraglacial lakes that drained in previous years (Morriss et al., 2013; Williamson et al., 2017). Theoretical subglacial hydraulic potential gradients, which may provide information about subglacial flow paths connecting discrete inputs to downglacier areas (Gulley et al., 2012), indicated our camp was located along the theoretical subglacial flow path draining these lakes (Figure 1). On 10 July 2018, we instrumented PIRA moulin with a pressure transducer to measure water pressure in the most connected subglacial drainage system (Andrews et al., 2014). We measured ice motion using three Global Navigation Satellite System (GNSS) stations spanning approximately 750 m in the across-flow direction from GNSS station JEME, positioned near our instrumented moulin. In May 2018, we installed a seismic station near PIRA moulin to measure seismic glacio-hydraulic tremor, a proxy for the subglacial flux of water within the most-connected regions of the subglacial drainage system (Bartholomaus et al., 2015), and the occurrence of icequakes associated with nearby ice fracture (Roeoesli et al., 2016). Finally, we use meteorological data from LOWC weather station (Mejia, Trunz, Covington, & Gulley, 2020), installed at our field site, filling in data gaps with data from the GC-NET (Steffen et al., 1996) weather station JAR1.

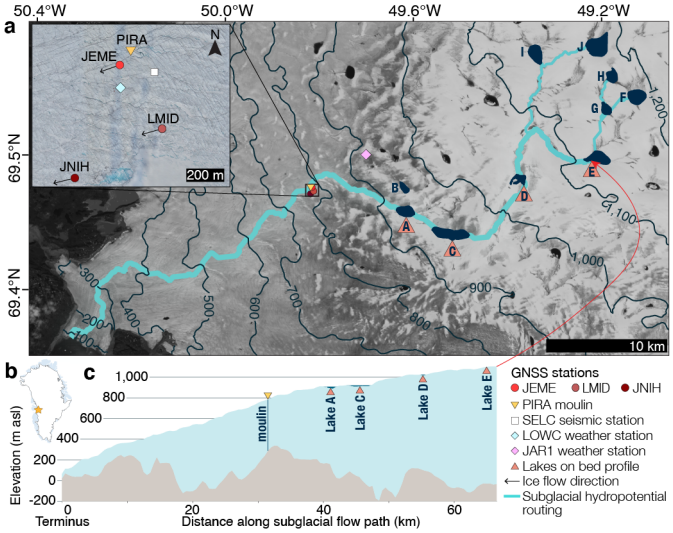

Figure 1. Study area in the Paakitsoq region of the Greenland Ice Sheet. a, Landsat-8 image (21 July 2018) of Sermeq Avannarleq with a July 2018 drone orthophoto shown in the study area zoom-in window. Site symbols are shown in the key. 100-m ice-surface elevation contours derived from BedMachine v3 (Morlighem et al., 2017) data. Maximum supraglacial lake extent filled in navy. b, Sermeq Avannarleq (yellow star) location. c, Surface and bed elevations along subglacial flow path extending from lake E to the terminus in cyan (Schwanghart & Kuhn, 2010)

2.2 Moulin Instrumentation

We instrumented moulins during the 2017 (JEME moulin, Supplementary Materials) and 2018 (PIRA moulin) melt seasons after the snowline had retreated past the site. In both years the upper 30 m of the moulins were visible and appeared vertical. We measured water pressures within each moulin using Geokon 4500HD-7.5MPa piezometers affixed to armored cable. Moulins were instrumented by lowering measured lengths of cable until the sensor reading increased with water depth, indicating we reached the water column within the moulin shaft. We then continued lowering the sensor while confirming depth increases. Upon encountering features where feeding more cable into the moulin did not change the sensor's recorded depth, we anchored the cable to the ice surface. We fixed the sensor in place within PIRA moulin at 154.5 m below the ice surface. We recorded water pressures every 15-minutes by Campbell Scientific CR-1000 data loggers equipped with AVW200 modules. We estimate an error of 20 m in our absolute moulin head measurements, arising from the uncertainty in the sensor elevation as described in detail by Andrews et al. (2014). Importantly, error in absolute moulin head does not apply to our measurements of relative change (e.g. diurnal variations) which should have an associated error on the order of centimeters.

2.3 Ice Motion and Uplift

We determined kinematic site positions from our GNSS stations (JEME, LMID, and JNIH) using TRACK software (Herring et al., 2010; Xie et al., 2019) which uses carrier-phase differential processing relative to bedrock mounted base stations. We use both GNSS stations KAGA (28 km baseline length) and ROCK (36 km baseline) as reference stations. We estimate kinematic positions using 30-second intervals that match our receiver sampling rates, we apply a 10-degree cutoff angle to reduce multi-path and use long baseline mode during processing. To minimize smoothing gaps at the boundaries of our daily

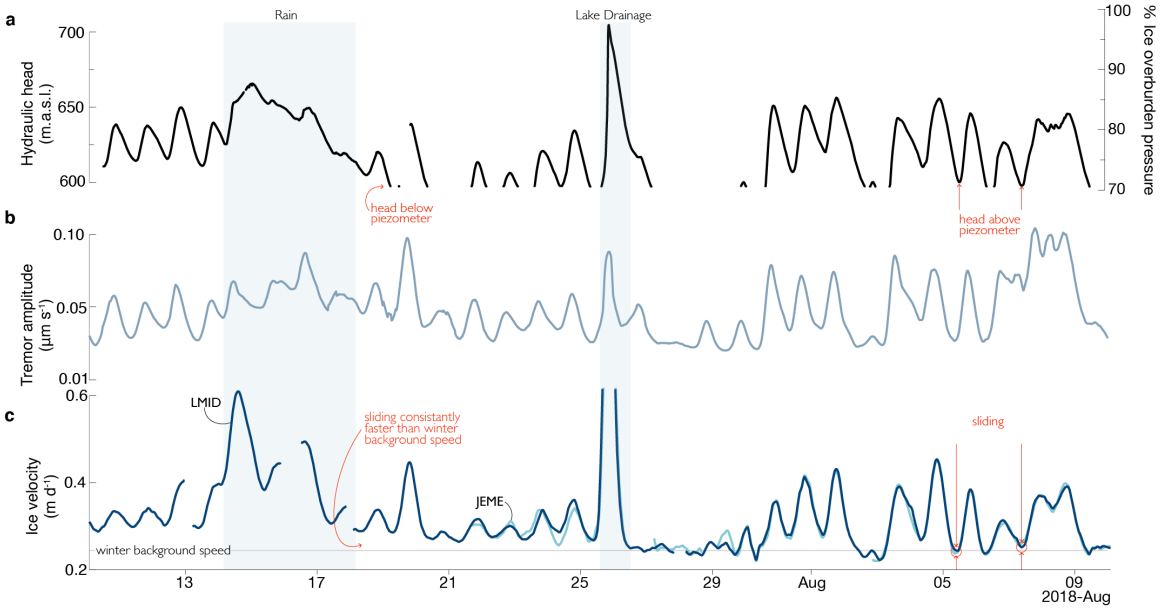

Figure 2. 2018 moulin hydraulic head, tremor amplitude, and ice velocity. a, PIRA moulin hydraulic head and as a percentage of ice overburden pressure. b, 6-h averaged glaciohydraulic tremor amplitude recorded at station SELC. c, 6-h averaged along-flow ice velocity of stations LMID (blue) and JEME (light blue). The timeseries is truncated to an upper limit of 0.6 m d^{-1} to preserve diurnal velocity minima. The full range of ice velocity (extending to 1.5 m d^{-1}) is shown in Figure 3. Gray line shows winter background speed at station LMID is 0.24 m d^{-1}. Shading in all panels corresponds to periods of heavy rainfall and the lake drainage event.

observation files, we extend each observation file with 12-hours from the surrounding days. Overlapping time periods are removed from the final position time series. The velocity and uplift calculations (Howat et al., 2008; Virtanen et al., 2020) are described in the Supplement to this paper.

2.4 Glaciohydraulic tremor and icequake record

We deployed a seismic station approximately 150 meters away from PIRA moulin in April 2018 to record local icequakes and seismic glaciohydraulic tremor amplitude, a proxy for the flux of subglacial discharge (Bartholomaus et al., 2015). This station was equipped with a Nanometrics Centaur digitizer connected to a Nanometrics Trillium Compact Posthole sensor re-installed on 12 July 2018, 1.1 m below the ice surface. We poured sand over the top of the seismometer at the time of installation to improve coupling between the sensor and surrounding ice. Ablation measurements from late July 2018 indicate that the sensor remained at least 0.5 m below the ice surface at the time supraglacial lake floodwaters passed beneath the sensor.

3 Results

Before the lake drainages in late July 2018, daily meltwater production induced clear diurnal variations in moulin hydraulic head, glaciohydraulic tremor amplitude, and ice velocity (Figure 2). Moulin hydraulic head was moderately variable, with minimum values falling below the piezometer elevation of 597 m.a.s.l. (below 73±12% of ice overburden pressure), and maximum values up to 666 m.a.s.l. (about 88±9% of overburden).

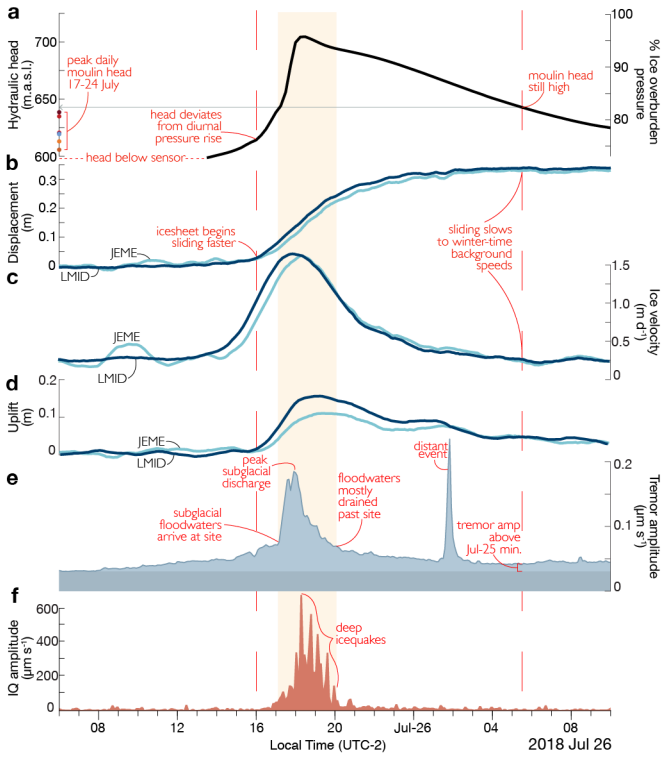

Figure 3. Coupled hydraulic, ice-dynamic, and seismic observations following the 2018 lake drainage event. a, PIRA moulin hydraulic head. b-d, GNSS station recordings from stations LMID (blue) and JEME (light blue). b, 30-minute filtered along-flow ice displacement detrended with respect to winter background motion. c, 2-h averaged along-flow ice velocity. d. 2-h averaged uplift from beginning of event. e, Glaciohydraulic tremor amplitude from seismic station SELC. f, Maximum icequake amplitude over 5-min time intervals. Red dashed lines mark the boundaries of the ice-dynamic response. Yellow shading marks when tremor amplitude suggests floodwaters were directly under our site.

Diurnal peaks in moulin water level and ice velocity were well correlated (Figure S4.), indicating PIRA moulin was well-connected to the most hydraulically-efficient regions of the subglacial drainage system that control sliding on sub-diurnal timescales (Andrews et al., 2014). Importantly, before the lake drainage event, ice velocity remained above wintertime background sliding speeds at all times, even when water levels dropped below the piezometer elevation (Figure 2; 19-23 July 2018).

Between 24-30 July 2018, Sentinel-2A and Landsat-8 imagery captured the drainage of ten supraglacial lakes located 8-26 kilometers up-glacier from our instrumented moulin (Fig. 1 Lakes A-J; Figure S1; Table S2). On 25 July at 16:00 local time, moulin water level, ice sliding speeds, and uplift began increasing faster than typical diurnal fluctuations marking the first disturbance to the connected drainage system (Fig. 3ab). An hour after the initial pressure perturbation, glaciohydraulic tremor amplitude sharply increased between 17:15-18:00, suggesting the abrupt arrival of subglacial floodwaters at our site (Fig. 3e). By 18:00, moulin water levels climbed 86 m, reaching 700 m.a.s.l. (approximately 95±7% of overburden). As moulin water levels were quickly rising, along-flow sliding speed peaked to 1.5 m d^{-1} at stations JEME and LMID (Fig. 3b), while the ice was uplifting most rapidly. Maximum event vertical displacement was 10±5 cm and 15±5 cm at JEME and LMID respectively (Fig. 3d). As the subglacial floodwave be-

gan to wane and moulin water levels stalled near their highest levels, we observed the onset of exceptionally high amplitude, frequent icequakes at 18:15 (Fig. 3f). Strong icequakes, interpreted to come from the ice sheet bed, continued as the ice sheet regrounded to the bed. By 20:00 moulin water levels and uplift were gradually declining, ice sliding was slowing down, icequake amplitude was getting smaller, and tremor amplitude had halved, all suggesting that most of the floodwaters had drained past our site. Over the next several hours, moulin water levels declined gradually. In contrast, sliding speeds slowed to winter background speeds (hereafter termed simply "background speeds") by 06:00 on 26 July, even though moulin water levels were still high. Further, similar tremor amplitudes before and after the lake drainage indicate that the subglacial channel's hydraulic capacity was unchanged (Fig. 3f), agreeing with previous modelling results (Dow et al., 2015). These observations demonstrate that pressure decreases within the most connected parts of the subglacial drainage system do not control ice velocity decreases. For this slowdown to occur, basal traction would need to increase over enough of the bed to counter the high-water pressures in the most connected parts of the drainage system.

For the remainder of the melt season, peak diurnal moulin water levels and sliding speeds remained well-correlated, but, in contrast to the period before the lake drainage, ice velocity minimums recurrently fell to background speeds (Fig. 2; Fig. S4). For example, before the lake drainage (19-25 July), moulin water level fell below the piezometer's 597 m.a.s.l. elevation while ice velocities remained above background speeds. However, after the lake drainage, ice velocity fell to background speeds while moulin water levels were above the piezometer (600 m.a.s.l. on 5 August and 598 m.a.s.l. on 7 August; Figure S4). This change in the relationship between diurnal minima indicates the increased basal traction triggered by the lake drainage has a lasting effect on ice velocity minima. We recorded a similar progression in 2017, but without seismic observations (Supplementary Materials).

4 Discussion

Given our observations before, during, and after lake drainages in 2017 and 2018, we infer that the slowdown to winter background speeds was caused by increased basal traction following the drainage of water from isolated cavities that became transiently connected during the lake drainage event and not increased channelization.

4.1 Conceptual Model of Flood wave Induced Isolated Cavity Connection

We interpret the results of our study to reflect the following sequence of events. Rapid lake drainage triggered a subglacial floodwave that quickly exceeded the subglacial drainage system's hydraulic capacity, as evidenced by rapid increases in moulin hydraulic head and ice motion as the floodwave approached our site (Fig. 3). As sliding speed increased, subglacial cavities expanded, forming new connections between linked and previously isolated cavities where cavities grew into each other (Fig. 4a-b). As the distributed drainage system expanded, high-pressure areas expanded across the bed to further increase sliding. Once the subglacial floodwave began to recede, back-pressure dissipated, allowing water injected into the distributed system to drain back towards conduits (Bartholomaus et al., 2007). Water within previously isolated cavities drained through newly formed connections, reducing water pressure within these previously high-pressure cavities (Fig. 4c). Drainage of isolated cavities, therefore, increased basal traction and slowed sliding to background speeds. After the lake drainage event, interconnections formed during the lake drainage event could have persisted, effectively expanding the distributed drainage system. Additionally, some connections may have closed closed-off when water pressures were low (Iken & Truffer, 1997; Murray & Clarke, 1995; Rada & Schoof, 2018), remaining below ice overburden pressure due to the slow timescales of internal meltwater gen-

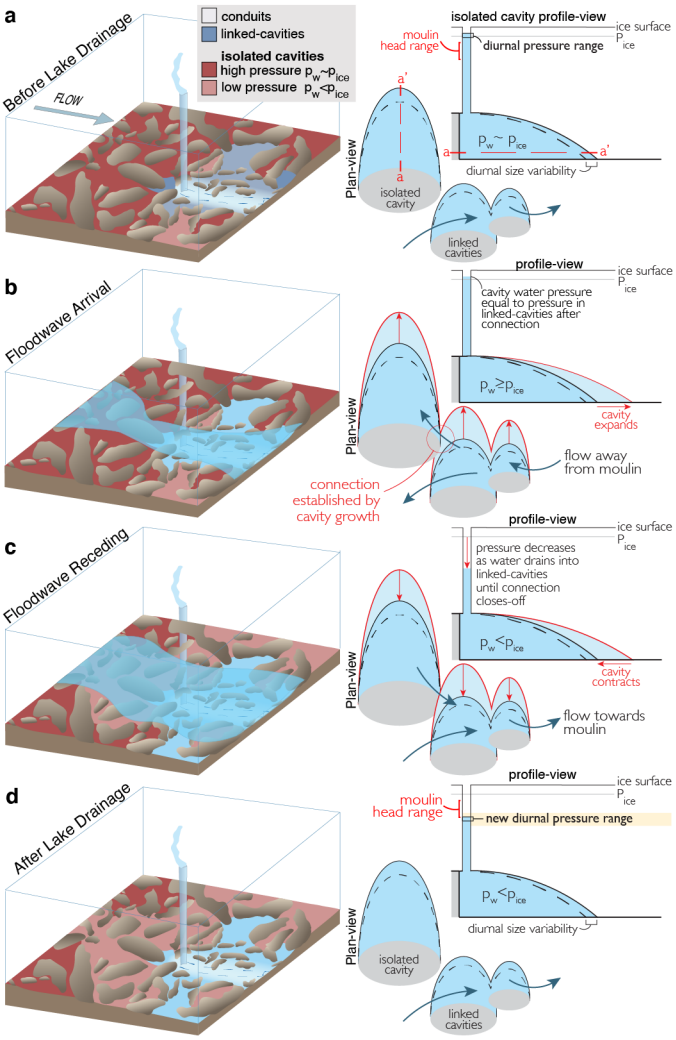

Figure 4. Conceptual model of rapid lake drainages dewatering isolated drainage system. a, Pre-lake drainage: meltwater inputs to moulins drain through subglacial conduits (blue dashed line) which exchange water with nearby linked-cavities (blue). High-pressure isolated cavities occupy a large fraction of the bed with pressure fluctuations opposing those in the connected drainage system. b, Rising limb of floodwave: floodwaters quickly overwhelm conduits, driving water laterally into the distributed system and ice accelerates. Cavities expand and grow into each other at which time water quickly fills and over pressurizes previously isolated cavities. c, Receding-limb of floodwave: water flows through new connections back towards conduits reducing water pressures over a large area of the bed. d, Post-lake drainage: linked-cavities and low-pressure isolated and weakly connected cavities occupy a larger area of the bed, increasing basal traction when compared to pre-lake drainage.

eration required to repressurize the cavity or by maintaining a "weak" connection to the distributed system (Hoffman et al., 2016). As such, a persistent basal traction increase would have been produced as long as most of the drained cavities remained at pressures below ice overburden pressure, resulting in the observed reoccurring slowdown to background sliding speeds.

4.2 Role of Rapid Lake Drainages on GrIS Sliding

While previous studies have emphasized the role of lakes in temporarily increasing sliding speeds, our study suggests rapid lake drainages can trigger rapid isolated cavity drainage following the passage of subglacial floodwaves. Consequently, the role of rapid lake drainages on ice dynamics is ambiguous. On the one hand, lake drainages increase ice velocities by triggering speedups (Selmes et al., 2011; Stevens et al., 2015) and creating stress conditions that form new moulins that deliver meltwater to the bed (Hoffman et al., 2018). On the other hand, our data show lake drainages can decrease ice velocities over large areas by dewatering isolated cavities, explaining the correlation between rapid lake drainages and the onset of seasonal ice deceleration (Andrews et al., 2018).

When compared to other work on isolated cavities on the GrIS (Andrews et al., 2014; Hoffman et al., 2016), our study suggests that seasonal ice dynamics and the onset of ice deceleration may vary depending on whether or not areas of the ice sheet are influenced by rapid lake drainages or only local inputs by moulins. In areas of the ice sheet that are influenced by rapid lake drainages, massive subglacial floodwaves can expand into and connect cavities across large areas of the bed. Dewatering of previously isolated cavities would then drive seasonal ice deceleration (Andrews et al., 2018), potentially early in the melt season. In areas of the ice sheet not influenced by rapidly draining lakes, short-lived increases in melting and meltwater delivery to moulins may create smaller scale, more local flood events that overwhelm the hydraulic capacity of the drainage system connected to a single moulin and drive either the incremental dewatering of isolated cavities or gradual drainage of weakly connected cavities (Andrews et al., 2014; Hoffman et al., 2016).

4.3 Role of Isolated Cavities in Driving GrIS Slowdowns

Neither rapid lake drainages nor the isolated drainage systems are currently considered in the models used to predict the GrIS's sea-level rise contribution. To a large degree, their lack of inclusion stems from the widespread use of alpine glaciers as GrIS analogues. While GrIS ice dynamics have long been interpreted in the context of better-studied alpine glaciers, there are essential differences between the two systems that may limit the applicability of the alpine glacier model to the GrIS. High moulin densities, steep surface slopes, thin ice, and slow creep-closure rates of smaller alpine glaciers allow for dense networks of high-capacity channels. High channel density can lower subglacial water pressure over broad regions of the glacier bed and limit the area available for isolated cavity formation, both of which limit the impacts of isolated cavities on alpine glacier sliding.

On the GrIS, however, low moulin densities likely result in lower subglacial channel density (Banwell et al., 2016), meaning there is more bed area available for isolated cavities to form and influence ice dynamics. Shallow surface slopes, thick ice, and fast creep-closure rates, characteristic of much of the GrIS ablation zone, may limit the drainage system's ability to increase its hydraulic capacity quickly enough to drain enough water from the distributed system and lower water pressure over large areas of the bed. Accordingly, GrIS dynamics may be more sensitive to sustained meltwater inputs than previously thought.

5 Conclusion

Direct measurements of water pressure along a subglacial flow-path showed that large influxes of meltwater from lake drainages can drain isolated cavities and slow sliding speeds without increasing the drainage system's efficiency. Building upon previous studies (Andrews et al., 2014; Hoffman et al., 2016), these results demonstrate that decreasing ice velocity has been mainly incorrectly attributed to the subglacial drainage system's ability to adjust its hydraulic capacity in response to meltwater inputs readily. As a result, ice dynamics of the GrIS may be especially vulnerable to sustained meltwater inputs, even where efficient subglacial drainage does exist. Future modelling efforts must incorporate the response of unchannelized parts of the subglacial drainage system to meltwater inputs in order to achieve accurate predictions of future GrIS contributions to sea-level rise.

Acknowledgments

This work was supported by the United States National Science Foundation grant number 1604022. The GNSS base station and on-ice stations were provided by UNAVCO in collaboration with N.S.F. Logistical support was provided by CH2MHill Polar Services. The authors declare there are no conflicts of interest with regard to finances or with the results of this paper. We thank Victoria Siegel, Charles Breithaupt, and others for their assistance in the field.

Data Availability Statement

The data associated with this manuscript can be accessed through the ArcticData.io platform [doi:10.18739/A2M03XZ13, doi:10.18739/A2CF9J745.], (Mejia, Trunz, Covington, Gulley, & Breithaupt, 2020; Mejia, Trunz, Covington, & Gulley, 2020).

References

Andrews, L. C., Catania, G. A., Hoffman, M. J., Gulley, J. D., Lüthi, M. P., Ryser, C., ... Neumann, T. A. (2014). Direct observations of evolving subglacial drainage beneath the Greenland Ice Sheet. *Nature*, *514*(7520), 80–83. Retrieved from `http://www.nature.com/doifinder/10.1038/nature13796` doi: 10.1038/nature13796

Andrews, L. C., Hoffman, M. J., Neumann, T. A., & Catania, G. A. (2018). Seasonal Evolution of the Subglacial Hydrologic System Modified by Supraglacial Lake Drainage in Western Greenland. *Journal of Geophysical Research : Earth Surface*, *123*, 1479–1496. doi: 10.1029/2017JF004585

Banwell, A. F., Hewitt, I. J., Willis, I. C., & Arnold, N. S. (2016). Moulin density controls drainage development beneath the Greenland ice sheet. *Journal of Geophysical Research: Earth Surface*, *121*(12), 2248–2269. doi: 10.1002/2015JF003801

Bartholomaus, T. C., Anderson, R. S., & Anderson, S. P. (2007). Response of glacier basal motion to transient water storage. *Nature Geoscience*, *1*, 33–37. doi: 10.1038/ngeo.2007.52

Bartholomaus, T. C., Larsen, C. F., Amundson, J. M., O'Neel, S., Walter, J. I., & West, M. E. (2015). Subglacial discharge at tidewater glaciers revealed by seismic tremor. *Geophysical Research Letters*, *42*, 6391–6398. doi: 10.1002/2015GL064590.Received

Bartholomew, I., Nienow, P. W., Sole, A. J., Mair, D., Cowton, T., & King, M. A. (2012). Short-term variability in Greenland Ice Sheet motion forced by time-varying meltwater drainage: Implications for the relationship between subglacial drainage system behavior and ice velocity. *Journal of Geophysical Research: Earth Surface*, *117*(3), 1–17. doi: 10.1029/2011JF002220,2012

Chandler, D. M., Wadham, J., Lis, G., Cowton, T., Sole, A. J., Bartholomew, I.,

... Hubbard, A. (2013). Evolution of the subglacial drainage system beneath the Greenland Ice Sheet revealed by tracers. *Nature Geoscience*, *6*(3), 195–198. Retrieved from http://dx.doi.org/10.1038/ngeo1737 doi: 10.1038/ngeo1737

Colgan, W. T., Rajaram, H., Anderson, R. S., Steffen, C., Zwally, H. J., Phillips, T., & Abdalati, W. (2011). The annual glaciohydrology cycle in the ablation zone of the Greenland ice sheet: Part 1. Hydrology model. *Journal of Glaciology*, *57*(204), 51–64. doi: 10.3189/2012JoG11J081

Dow, C. F., Kulessa, B., Rutt, I., Tsai, V. C., Pimentel, S., Doyle, S. H., ... Hubbard, A. (2015). Modeling of subglacial hydrological development following rapid supraglacial lake drainage. *Journal of Geophysical Research : Earth Surface*, *120*, 1127–1147. doi: 10.1002/2014JF003333.Received

Gulley, J. D., Grabiec, M., Martin, J. B., Jania, J., Catania, G. A., & Glowacki, P. S. (2012). The effect of discrete recharge by moulins and heterogeneity in flow-path efficiency at glacier beds on subglacial hydrology. *Journal of Glaciology*, *58*(211), 926–940. doi: 10.3189/2012JoG11J189

Herring, T., King, R. W., & McClusky, S. C. (2010). Introduction to GAMIT/GLOBK. *Mass. Inst. of Technol., Cambridge, Mass*.

Hoffman, M. J., Andrews, L. C., Price, S. F., Catania, G. A., Neumann, T. A., Lüthi, M. P., ... Morriss, B. (2016). Greenland subglacial drainage evolution regulated by weakly connected regions of the bed. *Nature Communications*, *7*, 13903. Retrieved from http://www.nature.com/doifinder/10.1038/ncomms13903 doi: 10.1038/ncomms13903

Hoffman, M. J., Catania, G. A., Neumann, T. A., Andrews, L. C., & Rumrill, J. A. (2011). Links between acceleration, melting, and supraglacial lake drainage of the western Greenland Ice Sheet. *Journal of Geophysical Research: Earth Surface*, *116*(4), 1–16. doi: 10.1029/2010JF001934

Hoffman, M. J., Perego, M., Andrews, L. C., Catania, G. A., Price, S. F., Lüthi, M. P., ... Johnson, J. V. (2018). Widespread Moulin Formation During Supraglacial Lake Drainages in Greenland. *Geophysical Research Letters*, *45*, 778–788. doi: 10.1002/2017GL075659

Howat, I. M., Tulaczyk, S. M., Waddlngton, E. D., & Björnsson, H. (2008). Dynamic controls on glacier basal motion inferred from surface ice motion. *Journal of Geophysical Research*, *113*(F3), F03015. Retrieved from http://doi.wiley.com/10.1029/2007JF000925 doi: 10.1029/2007JF000925

Iken, A., & Truffer, M. (1997). The relationship between subglacial water pressure and velocity of Findelengletscher, Switzerland, during its advance and retreat. *Journal of Glaciology*, *43*(144), 328–338. doi: 10.1017/CBO9781107415324.004

Lliboutry, L. A. (1968). Local friction laws for glaciers: A critical review and new openings. *Journal of Glaciology*, *23*(89), 67–95.

Meierbachtol, T. W., Harper, J. T., Humphrey, N. F., & Wright, P. J. (2016). Mechanical forcing of water pressure in a hydraulically isolated reach beneath Western Greenland's ablation zone. *Annals of Glaciology*, *57*(72), 62–70. doi: 10.1017/aog.2016.5

Mejia, J., Trunz, C., Covington, M. D., & Gulley, J. D. (2020). *Meteorological data from two on-ice weather stations at 780 and 950 m asl elevations in the ablation area of Sermeq Avannarleq, West Greenland from 2017-2018.* Arctic Data Center. Retrieved from https://arcticdata.io/catalog/view/doi%3A10.18739%2FA2CF9J745 doi: 10.18739/A2CF9J745.

Mejia, J., Trunz, C., Covington, M. D., Gulley, J. D., & Breithaupt, C. (2020). *Moulin hydrological measurements from Sermeq Avannarleq, West Greenland Ice Sheet from 2017-2018.* Arctic Data Center. Retrieved from https://arcticdata.io/catalog/view/doi:10.18739/A2M03XZ13 doi: 10.18739/A2M03XZ13.

Morlighem, M., Williams, C. N., Rignot, E., An, L., Arndt, J. E., Bamber, J. L., ... Zinglersen, K. B. (2017). BedMachine v3: Complete Bed Topography and Ocean Bathymetry Mapping of Greenland From Multibeam Echo Sounding Combined With Mass Conservation. *Geophysical Research Letters*, *44*(21), 051–11. doi: 10.1002/2017GL074954

Morriss, B. F., Hawley, R. L., Chipman, J. W., Andrews, L. C., Catania, G. A., Hoffman, M. J., ... Neumann, T. A. (2013). A ten-year record of supraglacial lake evolution and rapid drainage in West Greenland using an automated processing algorithm for multispectral imagery. *Cryosphere*, *7*(6), 1869–1877. doi: 10.5194/tc-7-1869-2013

Murray, T., & Clarke, G. K. C. (1995). Black-box modeling of the subglacial water system. *Journal of Geophysical Research: Solid Earth*, *100*(B6), 10231–10245. doi: 10.1029/95jb00671

Rada, C., & Schoof, C. (2018). Channelized, distributed, and disconnected: Subglacial drainage under a valley glacier in the Yukon Subglacial drainage controls on basal sliding View project Channelized, distributed, and disconnected: subglacial drainage under a valley glacier in the Yu. *The Cryosphere*, *12*, 2609–2636. Retrieved from `https://doi.org/10.5194/tc-12-2609-2018` doi: 10.5194/tc-12-2609-2018

Roeoesli, C., Helmstetter, A., Walter, F., & Kissling, E. (2016). Meltwater influences on deep stick-slip icequakes near the base of the Greenland Ice Sheet. *Journal of Geophysical Research : Earth Surface*, *121*, 223–240. doi: 10.1002/2015JF003601.Received

Ryser, C., Lüthi, M. P., Andrews, L. C., Catania, G. A., Funk, M., & Hawley, R. L. (2014). Caterpillar-like ice motion in the ablation zone of the Greenland ice sheet. *Journal of Geophysical Research : Earth Surface*, *119*, 2258–2271. doi: 10.1002/2013JF003067.Received

Schwanghart, W., & Kuhn, N. J. (2010). TopoToolbox: A set of Matlab functions for topographic analysis. *Environmental Modelling and Software*. doi: 10.1016/j.envsoft.2009.12.002

Selmes, N., Murray, T., & James, T. D. (2011). Fast draining lakes on the Greenland Ice Sheet. *Geophysical Research Letters*, *38*(15), 1–5. doi: 10.1029/2011GL047872

Sole, A. J., Nienow, P. W., Bartholomew, I., Mair, D., Cowton, T., Tedstone, A. J., & King, M. A. (2013). Winter motion mediates dynamic response of the Greenland Ice Sheet to warmer summers. *Geophysical Research Letters*, *40*(15), 3940–3944. doi: 10.1002/grl.50764

Steffen, C., Box, J. E., & Abdalati, W. (1996). Greenland Climate Network: GC-Net. *Cold Regions Research and Engineering Laboratory*, *CRREL Spec*, 98–103.

Stevens, L. A., Behn, M. D., McGuire, J. J., Das, S. B., Joughin, I., Herring, T., ... King, M. a. (2015). Greenland supraglacial lake drainages triggered by hydrologically induced basal slip. *Nature*, *522*(7554), 73–76. Retrieved from `http://www.nature.com/doifinder/10.1038/nature14480` doi: 10.1038/nature14480

Stone, D., & Clarke, G. K. C. (1996). in Situ Measurements of Basal Water Quality and Pressure As an Indicator of the Character of Subglacial Drainage Systems. *Hydrological Processes*, *10*(4), 615–628. doi: 10.1002/(sici)1099-1085(199604)10:4⟨615::aid-hyp395⟩3.3.co;2-d

Sundal, A. V., Shepherd, A., Nienow, P. W., Hanna, E., Palmer, S., & Huybrechts, P. (2011). Melt-induced speed-up of Greenland ice sheet offset by efficient subglacial drainage. *Nature*, *469*(7331), 521–524. Retrieved from `http://dx.doi.org/10.1038/nature09740` doi: 10.1038/nature09740

Virtanen, P., Gommers, R., Oliphant, T. E., Haberland, M., Reddy, T., Cournapeau, D., ... Vázquez-Baeza, Y. (2020). SciPy 1.0: fundamental algo-

rithms for scientific computing in Python. *Nature Methods*, *17*, 261–272. doi: 10.1038/s41592-019-0686-2

Walder, J. S. (1986). Hydraulics of subglacial cavities. *Journal of Glaciology*, *32*(112), 439–445. Retrieved from `http://www.igsoc.org:8080/journal/32/112/igs_journal_vol32_issue112_pg439-445.pdf`

Williamson, A. G., Arnold, N. S., Banwell, A. F., & Willis, I. C. (2017). A Fully Automated Supraglacial lake area and volume Tracking ("FAST") algorithm: Development and application using MODIS imagery of West Greenland. *Remote Sensing of Environment*, *196*, 113–133. Retrieved from `https://doi.org/10.1016/j.rse.2017.04.032` doi: 10.1016/j.rse.2017.04.032

Xie, S., Law, J., Russell, R., Dixon, T. H., Lembke, C., Malservisi, R., ... Chen, J. (2019). Seafloor Geodesy in Shallow Water With GPS on an Anchored Spar Buoy. *Journal of Geophysical Research: Solid Earth*, *124*(11), 12116–12140. doi: 10.1029/2019JB018242